Supplementary Information for

Catalytic Peptide-based Coacervates for Enhanced Catalytic Function through Structural Organization and Substrate Specificity

David Q. P. Reis [1], Sara Pereira[1], Ana P. Ramos[1], Pedro M. Pereira[1], Leonor Morgado[2,3], Joana Calvário[1], Adriano O. Henriques[1], Mónica Serrano[1] and Ana S. Pina[1*]

[1] Instituto de Tecnologia Química e Biológica António Xavier, Universidade Nova de Lisboa, Av. da República, 2780-157 Oeiras, Portugal

[2] Associate Laboratory i4HB - Institute for Health and Bioeconomy, NOVA School of Science and Technology, Universidade NOVA de Lisboa, 2829-516 Caparica, Portugal

[3] UCIBIO – Applied Molecular Biosciences Unit, Chemistry Department, NOVA School of Science and Technology, Universidade NOVA de Lisboa, 2829-516 Caparica, Portugal

*Correspondence and requests for materials should be addressed to A.S.P. (ana.pina@itqb.unl.pt)

Table of Contents:

1. Supplementary Materials

P7 peptide with 98.0% purity was purchased from Caslo. The salts to be used in buffered and chemical solutions were obtained from Fisher Bioreagents. The microscopy material was obtained from Avantor, Zeiss and IBIDI. DAPI (4',6-diamidino-2-phenylindole), FITC (3',6'-dihydroxy-6-isothiocyanatospiro[2-benzofuran-3,9'-xanthene]-1-one), TMR (tetramethylrhodamine), BSAp (phosphorylated Bovine Serum Albumin, FITC-Labelled BSA - P3967, Human microtubule associated protein tau, Tau-441 - T0576, Tau-44p - TTBK1-Phosphorylated - SRP0695, FluoroTagTM FITC conjugation kit, QuantiProTM BCA Assay Kit., *p*-nitrophenyl phosphate (*p*NPP) were purchased from Sigma-Aldrich. Alexa Fluor™ 488 Microscale Protein Labeling Kit was ordered from ThermoFisher Scientific. Pluronics was purchased from Panreac, AppliChem. The 2′-[2-benzothiazoyl]-6′-hydroxybenzothiazole phosphate (BBTP), the commercially available AttoPhos® was obtained from Promega. The GFP (Green Fluorescent Protein) was purchased from Invitrogen.

2. Supplementary Methods

2.1 Study of the temperature and time during peptide-induced coacervation

Influence of the temperature in coacervation: To assess the effect of temperature on coacervation, the same protocol "Coacervation" as in supplementary note 2 was followed with variations in the incubation temperature. Different temperatures were employed ranging from 23°C to 37°C. By comparing the results obtained at these different temperatures, we aimed to evaluate the temperature-dependent influence on the coacervation phenomenon and its potential implications for the formation and stability of coacervate droplets.

Time-course coacervation: To investigate the dynamics of coacervation over time, we performed a comprehensive monitoring of the process at specific time intervals: 0, 1, 4, and 6 hours. Optical brightfield microscopy was utilized to observe the coacervation phenomenon in real-time. For this study, we selected the sample condition that exhibited optimal coacervate size and abundance, which involved a stock concentration of 5 mg mL^{-1} P7 peptide in 100 mM sodium phosphate buffer (pH 8.0) with a NaCl concentration of 1.00 M. The sample was initially incubated at a controlled temperature of 27°C (±1°C) for 1 hour. Subsequently, it was maintained at room temperature (23°C ± 2°C) for a total duration of 6 hours. By observing the coacervation process at different time points, we aimed to gain insights into the temporal evolution of coacervate formation, size, and stability, providing valuable information on the kinetics and dynamics of the coacervation process.

2.2 Partitioning of the p-Nitrophenyl Phosphate (pNPP) inside the coacervates

The partitioning efficiency of the substrate pNPP inside the coacervates was investigated and for this the absorbance spectra of pNPP were analyzed, revealing a peak at 312 nm (Fig. S17).

pNPPAbsorbance Spectra: A solution of 275 µL of 100 mM sodium phosphate with 1 M NaCl at pH 8.0 was prepared. To this, 25 µL of pNPP was added to achieve a final concentration of 0.1 mM, with a pNPP to solution ratio of 1:12. The sample's absorbance was then measured using the

INFINITE M NANO+ TECAN microplate reader, scanning from 250 to 450 nm. A distinct absorbance peak was observed at 312 nm, corresponding to the pNPP absorbance.

The partitioning protocol was then performed as described in the "Partitioning Experiments" section for the different final concentrations of pNPP (1-20 mM) used in the kinetic experiments.

3. Supplementary Notes

3.1 Study of the reversibility of the coacervation upon aggregation

Initially, a stock peptide solution with a concentration of 10 mg mL^{-1} was prepared in the presence of 1.00 M NaCl by following the coacervation with the partitioning protocol with FITC. Subsequently, this concentrated peptide solution was diluted to achieve a final P7 concentration of 5 mg mL^{-1} containing the same NaCl concentration. Upon dilution, we observed the dissolution of the aggregates and the rapid formation of coacervates. This experimental result provides compelling evidence for the reversible nature of coacervation, which is governed by the process of dilution. Figure S2 visually represents the sequential stages of dilution-induced coacervate formation, highlighting the dynamic and reversible behavior of the coacervation process.

4. Supplementary Tables 1-3

Supplementary Table 1 – P7 assigned backbone chemical shifts in the soluble and undergoing LLPS states. The chemical shifts were used for determination of the secondary structure elements represented in Supplementary Figure 7.

Residue	P7 soluble				P7 LLPS			
	HA	CA	CB	HN	HA	CA	CB	HN
K1	3,710	56,59	35,44	-	3,554	56,51	35,58	-
V2	4,129	62,23	32,70	-	4,060	62,08	32,87	-
Y3	4,610	-	39,44	-	4,542	57,72	39,33	-
F4	4,700	-	40,14	-	4,638	-	40,14	-
S5	4,469	55,36	63,99	-	4,403	55,39	63,90	-
I6	4,437	58,89	38,84	8,147	4,393	58,85	38,81	-
P7	4,455	63,36	32,01	-	4,390	63,41	31,98	-
W8	4,723	-	29,56	7,950	4,651	57,27	29,42	7,997
R9	4,324	55,64	31,33	-	4,255	55,54	31,24	-
V10	4,284	60,18	32,96	8,042	4,212	60,09	32,85	8,001
P11	4,449	63,57	32,21	-	4,367	63,25	31,95	-
M12	4,474	58,30	32,25	-	4,401	58,02	32,07	-

Supplementary Table 2 – Vibrational frequencies (cm^{-1}) of the absorption bands associated with secondary structure conformation of the various states of P7 in the Amide I band.

Assembly state	Vibrational frequency range (cm^{-1})	Maximum Peak (cm^{-1})	Structural assignment
Soluble (P7 1mg/mL with no sal)t	1597-1609	1605	Side chain moieties
	1634-1650	1640	Random Coil
	1679-1687	1685	β-turn
LLPS (P7 5mg/mL 1M NaCl)	1622-1631	1622	β-sheet
	1643-1648	1646	Random coil
	1660-1667	1663	β-sheet
	1679-1689	1683	β-turns
Aggregated (P7 10mg/mL 1M NaCl)	1618-1630	1623	β-sheet
	1633-1648	1640	Random Coil

Supplementary Table 3- Isoelectric points of the P7 and the proteins used in the affinity-mediated molecular uptake study

Proteins	**Isoelectric Point**
P7 peptide	11.46 (estimated by using Pepcalc tool)
BSA	5.6-6 (at pH 8 is intrinsically negative)
Tau	6.25 (at pH 8 is intrinsically negative)
CotB	9.83 (at pH 8 is intrinsically positive)
CotBp	4.51

5. Supplementary Figures 1-24

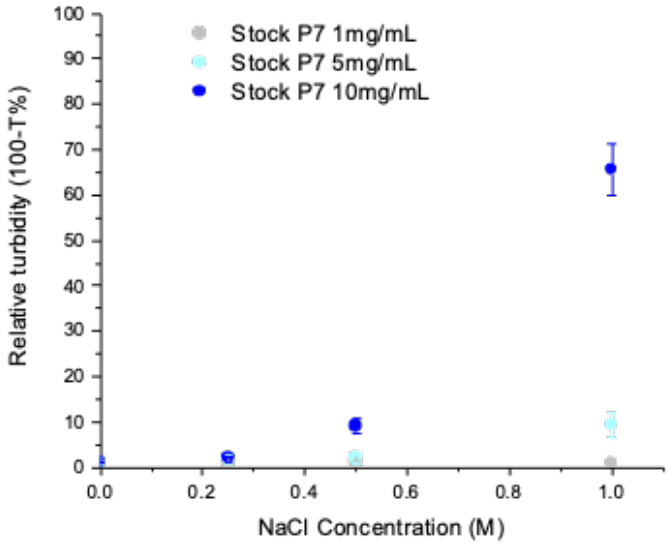

Supplementary Figure 1 – Turbidity measurements of the different stock P7 peptide concentrations (1 mg mL^{-1}, 5 mg mL^{-1} and 10 mg mL^{-1}) as a function of ionic strength. Data are presented as mean values ± SD (n=2) from two independent experiments.

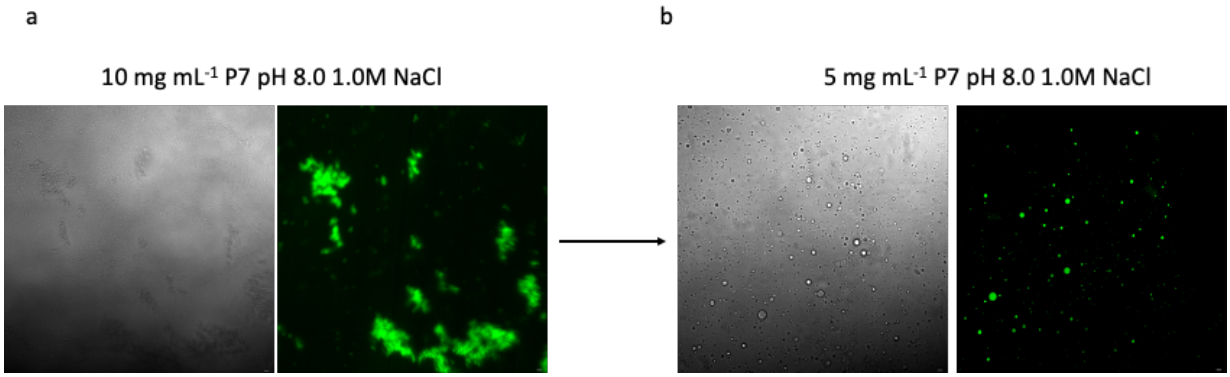

Supplementary Figure 2 - Reversible coacervation upon dilution of peptide aggregates (in the presence of FITC) from the condition a) stock 10 mg mL^{-1} P7 pH 8.0 1.0M NaCl to b) 5 mg mL^{-1} P7 pH 8.0 1.0M NaCl. Scale bar set to 10 μm. The confocal images are representative images from at least three independently samples with similar results.

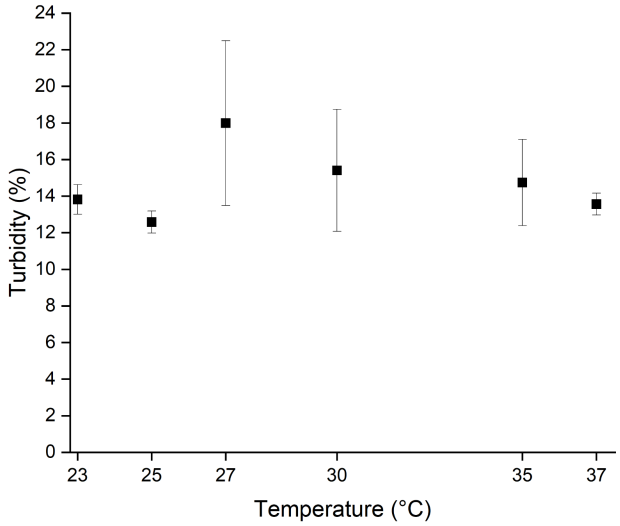

Supplementary Figure 3 - Turbidity measurements of the stock P7 peptide concentration of 5 mg mL^{-1}, pH 8.0, and 1.0 M NaCl, 1h coacervation as a function of the temperature. Data are presented as mean values ± SD (n=3) from three independent experiments.

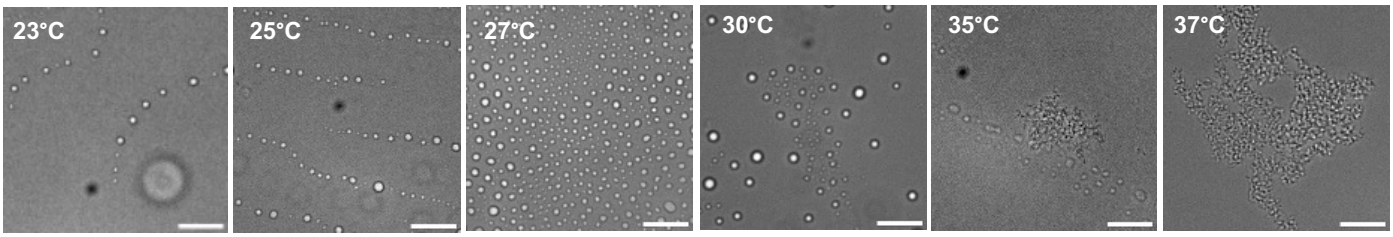

Supplementary Figure 4 - Influence of temperature ranging from 23°C to 37°C on coacervation formation using a stock P7 peptide concentration of 5 mg mL^{-1}, pH 8.0, and 1.0 M NaCl, for 1h. The scale bar is set to 10 μm. The microscopy images are representative images from at least three independently samples with similar results.

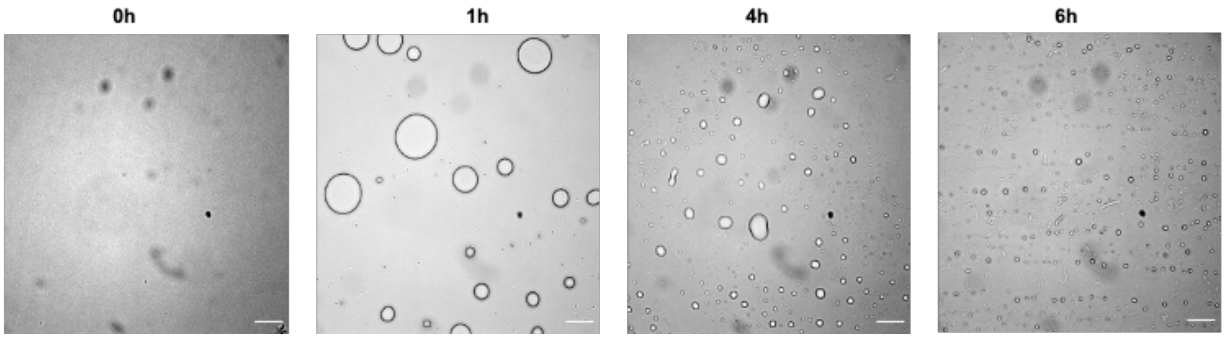

Supplementary Figure 5 - Time-course coacervation formation by brightfield optical microscopy. Sample condition of stock peptide concentration 5 mg mL^{-1} P7 in 100mM sodium phosphate buffer solution pH=8 1.00M of NaCl at different time points (0, 1, 4 and 6 hours). Scale bar set to 10μm. The microscopy images are representative images from at least three independently samples with similar results

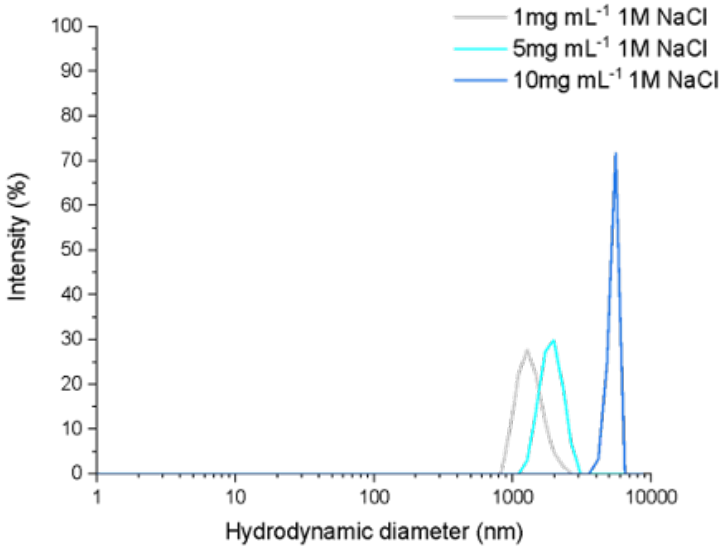

Supplementary Figure 6: Size of the coacervates measured by DLS at different conditions soluble with low turbidity and low amount of coacervates (stock P7 concentration: 1 mg mL^{-1} 1M in 100 mM sodium phosphate pH 8.0 1M NaCl), undergoing LLPS (stock P7 concentration: 5 mg mL^{-1} in 100 mM sodium phosphate pH 8.0 1M NaCl), and in the aggregated form (dark blue, stock P7 concentration: 10 mg mL^{-1} in 100 mM sodium phosphate pH 8.0 1M NaCl). Data are presented as mean values ± SD (n=3) from three independent experiments.

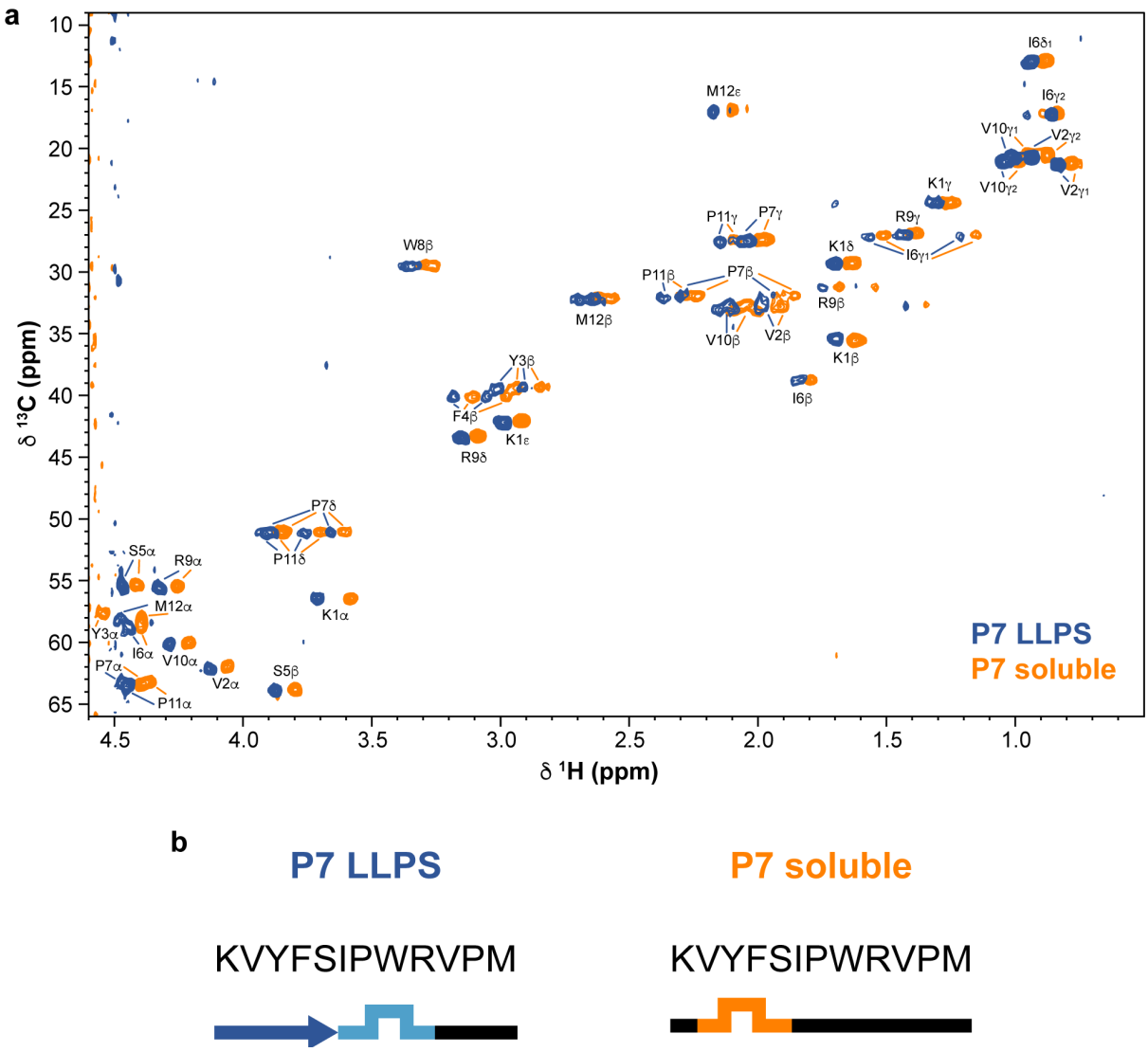

Supplementary Figure 7 – NMR studies on P7 coacervation. (a) 2D $^{1}H,^{13}C$ HSQC spectra and assignments for the two conditions analyzed: P7 peptide in a stock concentration of 5mg mL^{-1} in 100mM sodium phosphate buffer with no salt (soluble, in orange) and 1 M of NaCl at pH 8.0 (undergoing LLPS, in blue); (b) secondary structure graph as determined by CSI 3.0 web server with the backbone chemical shifts shown in Table S1.

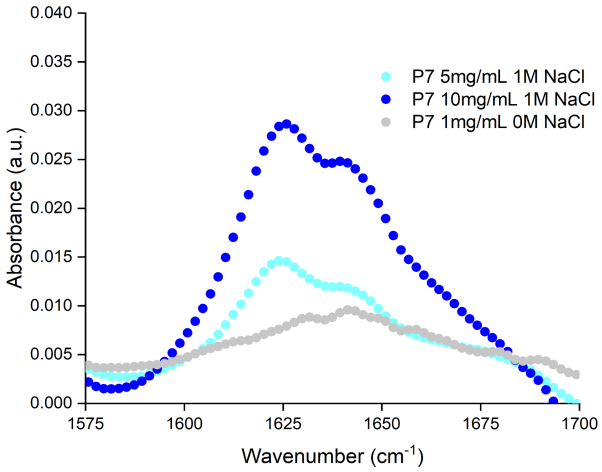

Supplementary Figure 8: FTIR spectra of the peptide in three distinct assembly states: soluble (1 mg mL^{-1}, undergoing LLPS (5 mg mL -1 1M NaCl), and in the aggregate (10 mg ml-1 1M NaCl)

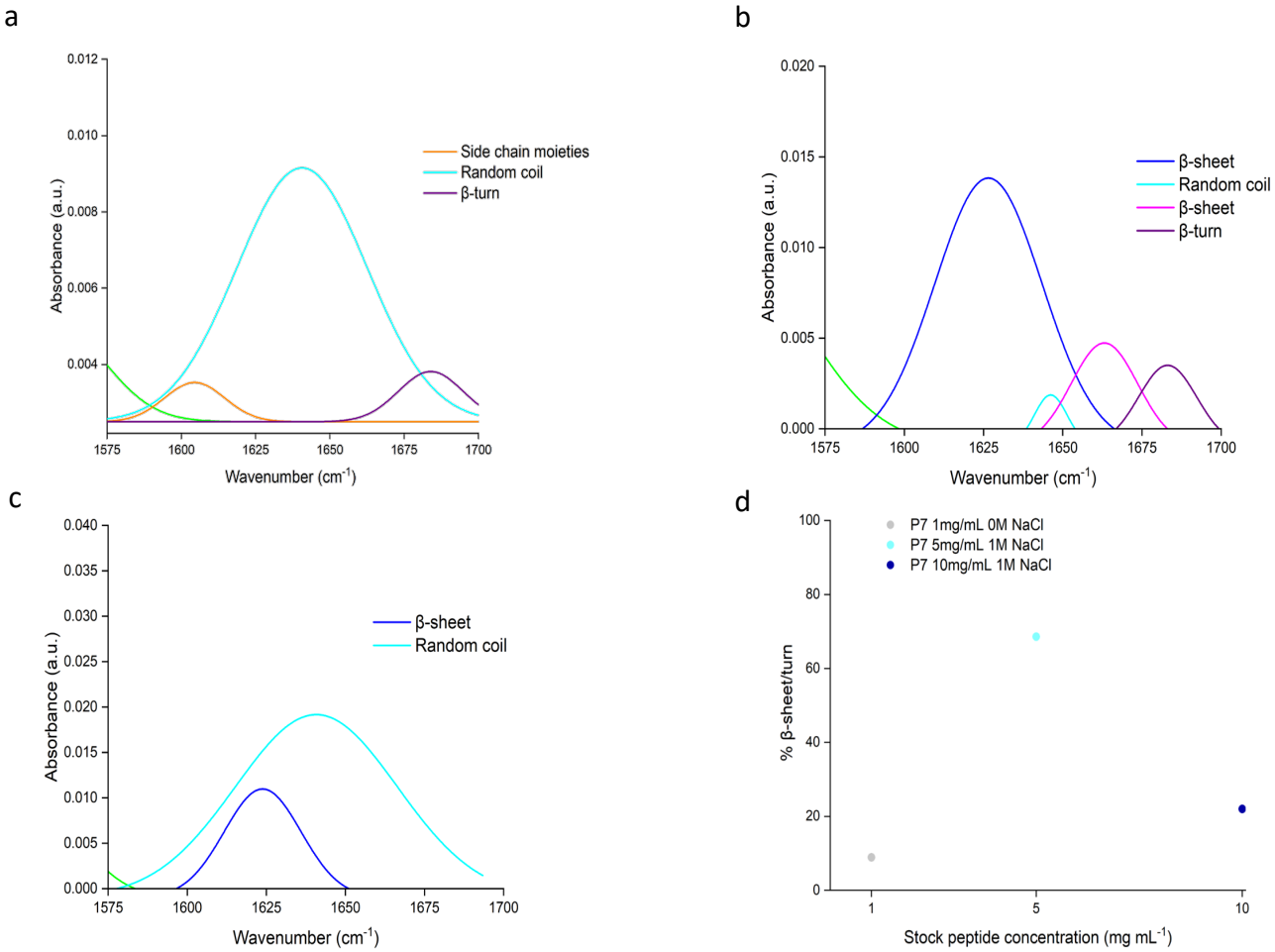

Supplementary Figure 9: Deconvolution of the amide band I peak of P7 in the various states: (a) soluble state (P7 stock concentration 1 mg mL^{-1} with no salt), (b) undergoing LLPS (stock concentration 5 mg mL^{-1} 1M NaCl) and, (c) aggregated state (10 mg ml-1 1M NaCl). (d) Percentage of β-sheet and β-turn content in the different assembly states, calculated from the areas

of peaks corresponding to β-sheet (1623 cm^{-1} and 1663 cm^{-1}) and β-turn (1683 cm^{-1}) structures, divided by the total area of all peaks in the amide I region.

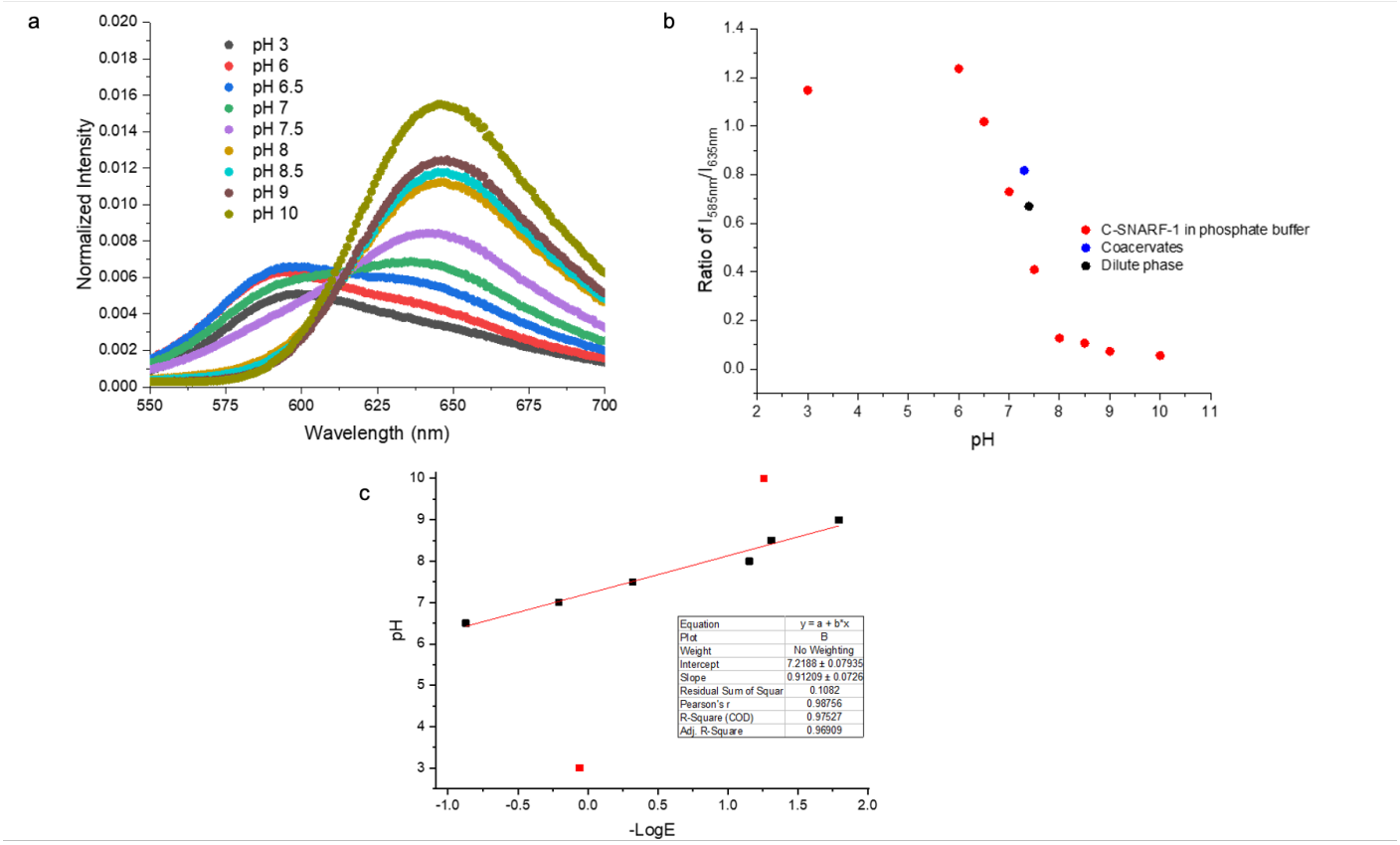

Supplementary Figure 10: Calibration methods of SNARF to estimate local apparent pH. (a) The fluorescence spectra of SNARF collected across a range of pH values. (b) Ratio of SNARF intensity at 585 nm and 635 nm as a function of pH changes. (c) pH calibration curve for SNARF-1 fluorescence. The pH is plotted against -logE, where E = (R-RB) / (RA-R). R represents the ratio of SNARF-1 fluorescence intensities at 585 nm and 635 nm. RA and RB are the ratio of SNARF fluorescence intensity at 585 nm and 635 nm at acidic and basic pH extremes, respectively. pH estimation was performed following established protocols

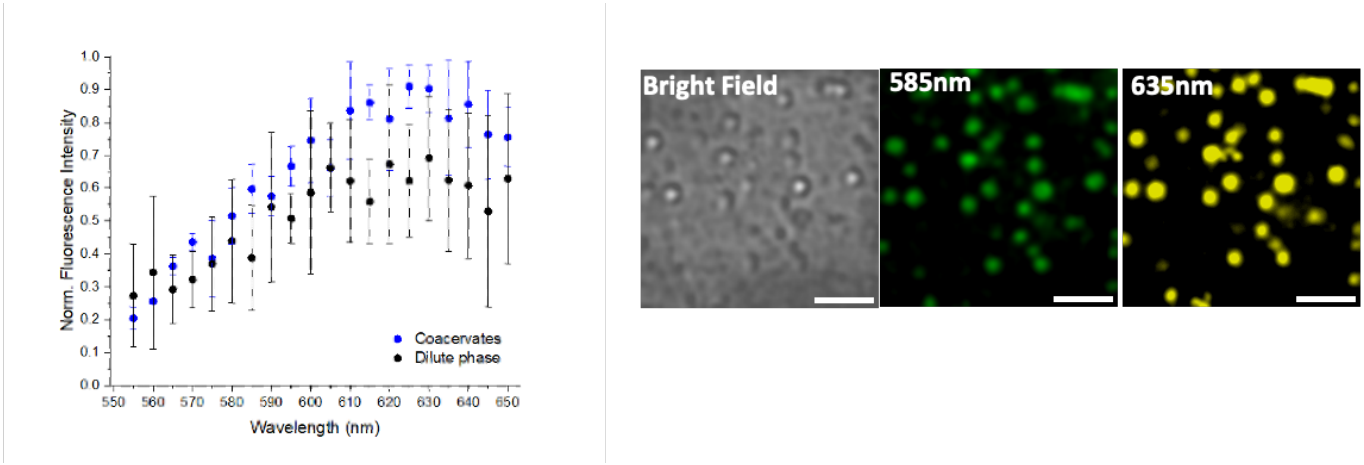

Supplementary Figure 11: Confocal images and lambda scan of SNARF in coacervate droplets. SNARF emission spectrum in coacervate droplets and dilute phase are measured by confocal microscope simultaneously and used to estimate the local apparent pH of SNARF. Data are presented as mean values ± SD (n=3) from three independent samples. The confocal microscopy images are representative images from at least three independently samples with similar results

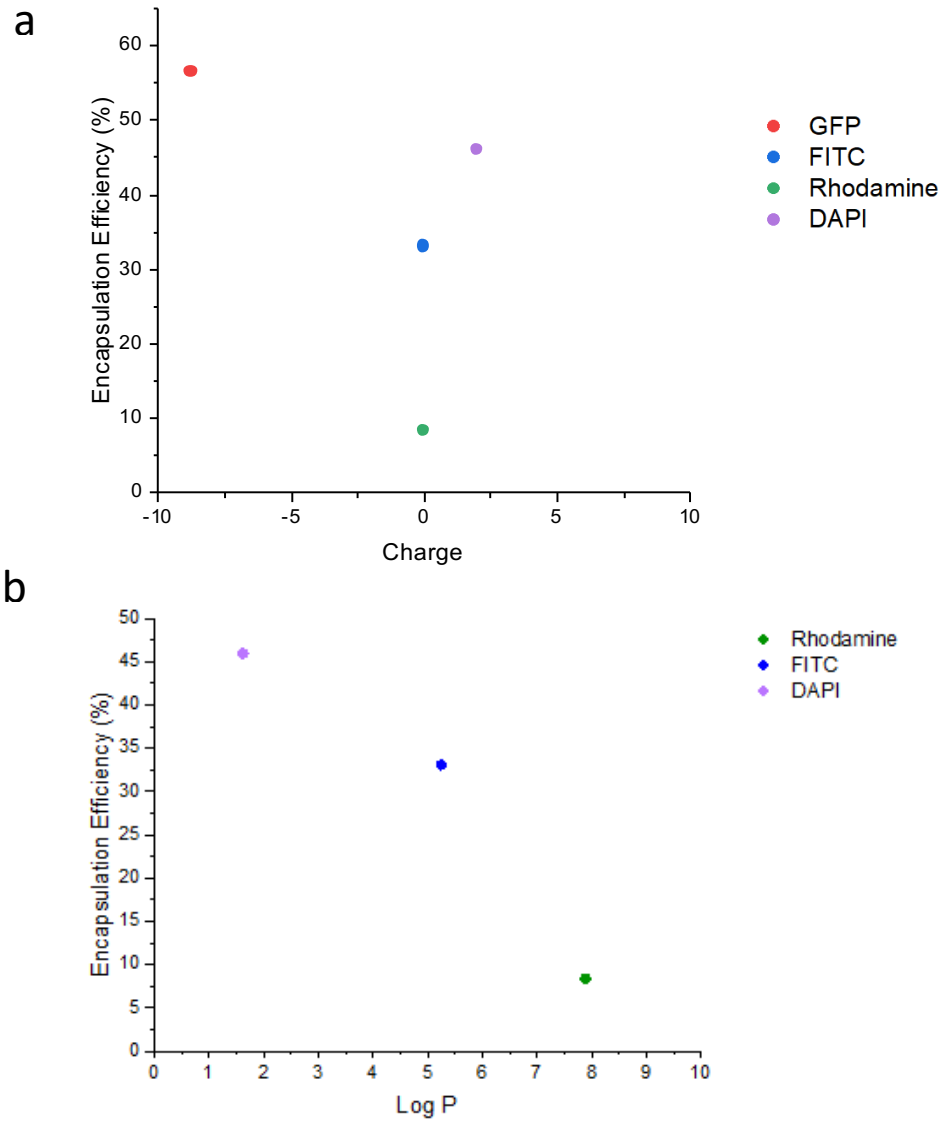

Supplementary Figure 12 - Influence of (a) charge and (b) LogP in the partitioning of the guest molecules in P7 coacervates. Data are presented as mean values ± SD (n=3) from three independent experiments.

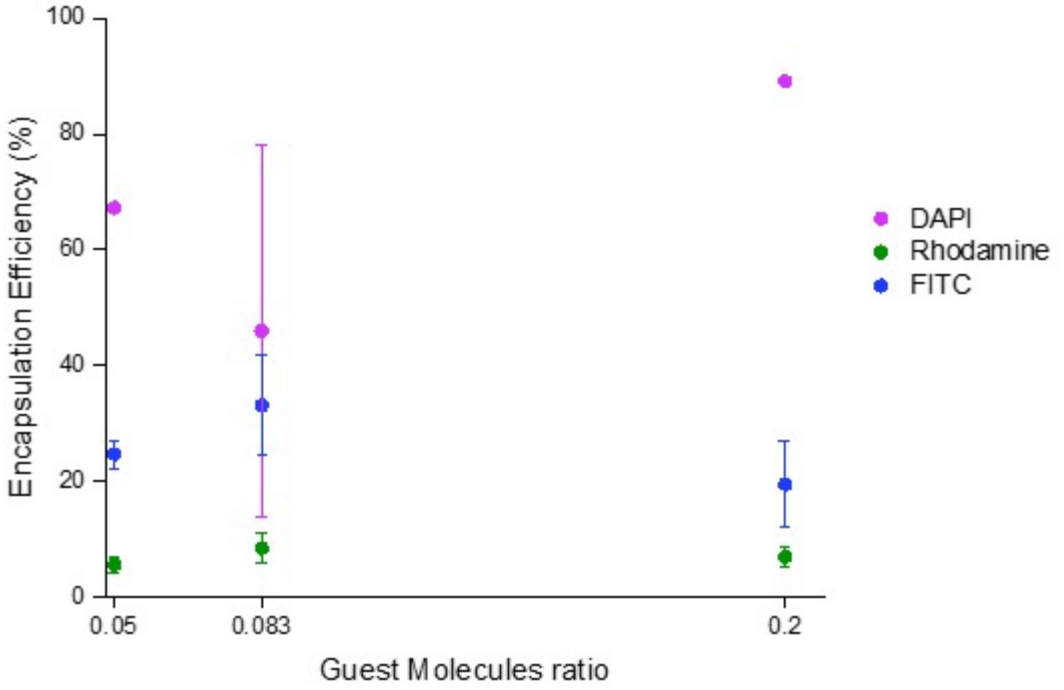

Supplementary Figure 13 – Encapsulation efficiency (%) of guest molecules as a function of the peptide-to-guest molecule ratio in P7 coacervates. Different peptide-to-guest molecule ratios were tested, including 1:5, 1:12, and 1:20. The encapsulation efficiency was determined by measuring the partitioning of the guest molecules within the coacervates. Data are presented as mean values ± SD (n=3) from three independent experiments.

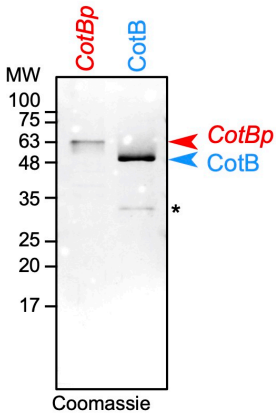

Supplementary Figure 14. SDS-PAGE analysis of purified CotB*p* and CotB-46. The recombinant proteins were overproduced in *E. coli* BL21(DE3) by autoinduction. CotB*p*, the hyperphosphorylated form of CotB was produced in the presence of the CotH kinase and the facilitator protein CotG [1]. Note that hyperphosphorylated CotB*p* migrates at around 66 kDa, while the unphosphorylated protein migrates close to the predicted size of 46 kDa. CotB and CotB*p* were purified by Ni^{2+}-affinity chromatography and analysed by 12.5% SDS-PAGE as previously described[1]. The blue arrow show the position of CotB*p* and the green arrow the position of CotB. Note that the phosphorylated CotB*p* stains less efficiently than CotB with Coomassie. The asterisk

indicates possible degradation forms of CotB. The position of the molecular weight markers (MW, in kDa) is indicated on the left side of the panel.

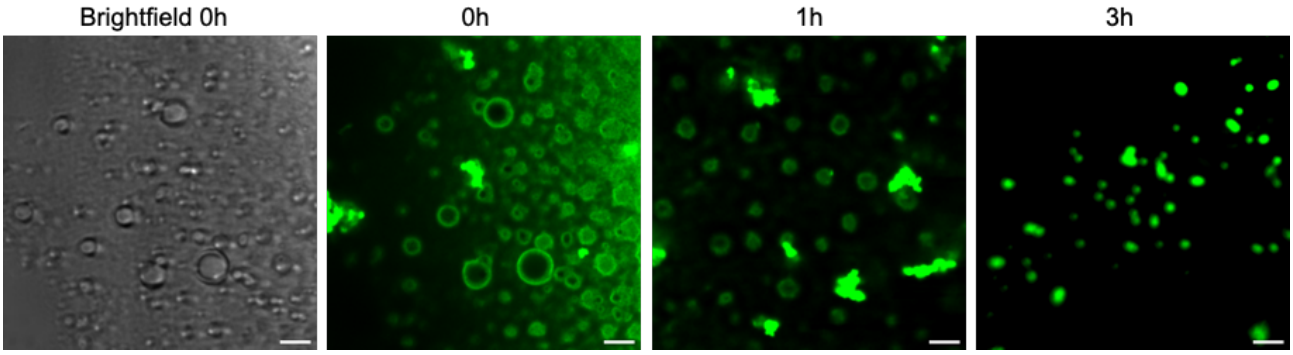

Supplementary Figure 15 – Full field of view of fluorescence confocal images at different timepoints following incubation of the P7 coacervates with FITC-labelled BSA*p*, Scale bar set to 10µm. The confocal microscopy images are representative images from at least three independently samples with similar results.

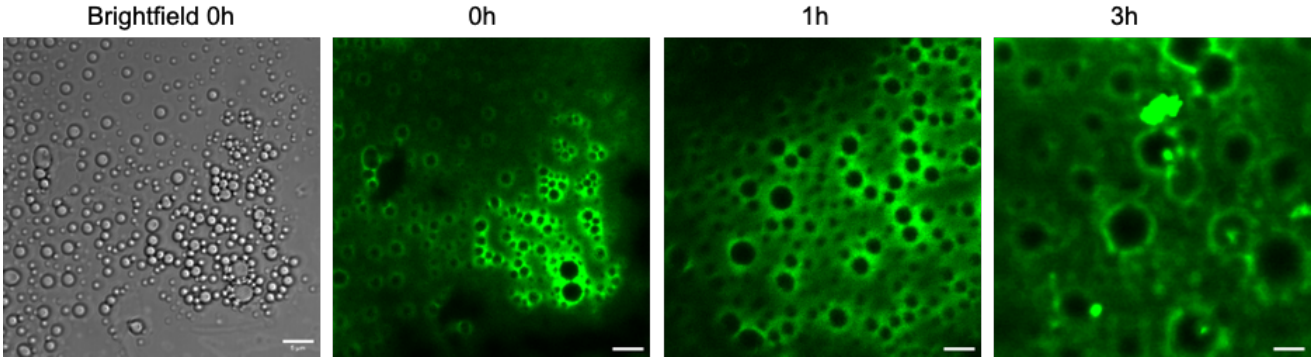

Supplementary Figure 16– Full field of view of fluorescence confocal images at different timepoints following incubation of the P7 coacervates with FITC-labelled BSA. Scale bar set to 10µm. The confocal microscopy images are representative images from at least three independently samples with similar results.

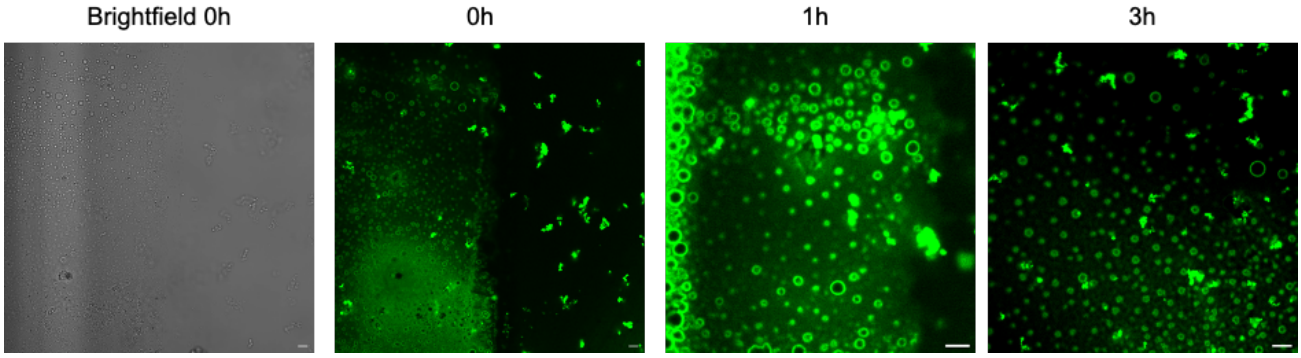

Supplementary Figure 17 – Full field of view of fluorescence confocal images at different timepoints following incubation of the P7 coacervates with ALEXA-labelled Tau*p*. Scale bar set to 10µm. The confocal microscopy images are representative images from at least three independently samples with similar results.

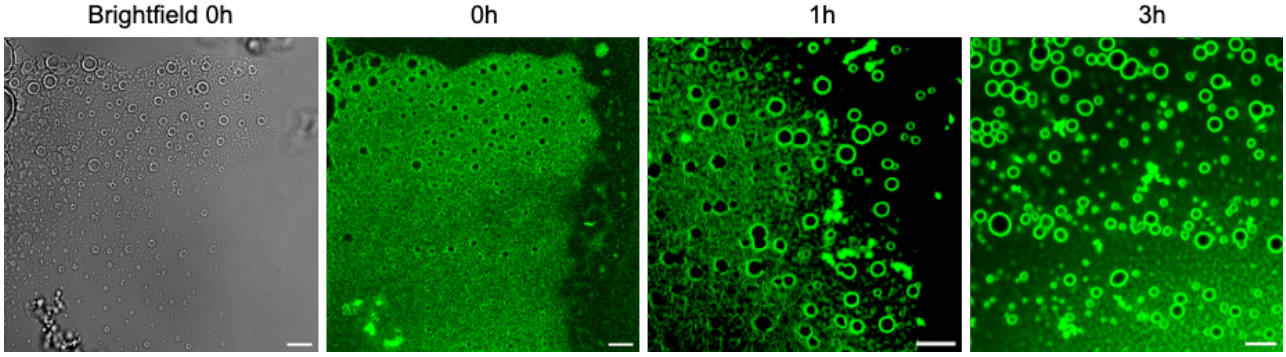

Supplementary Figure 18 – Full field of view of fluorescence confocal images at different timepoints following incubation of the P7 coacervates with ALEXA-labelled Tau. Scale bar set to 10µm. The confocal microscopy images are representative images from at least three independently samples with similar results.

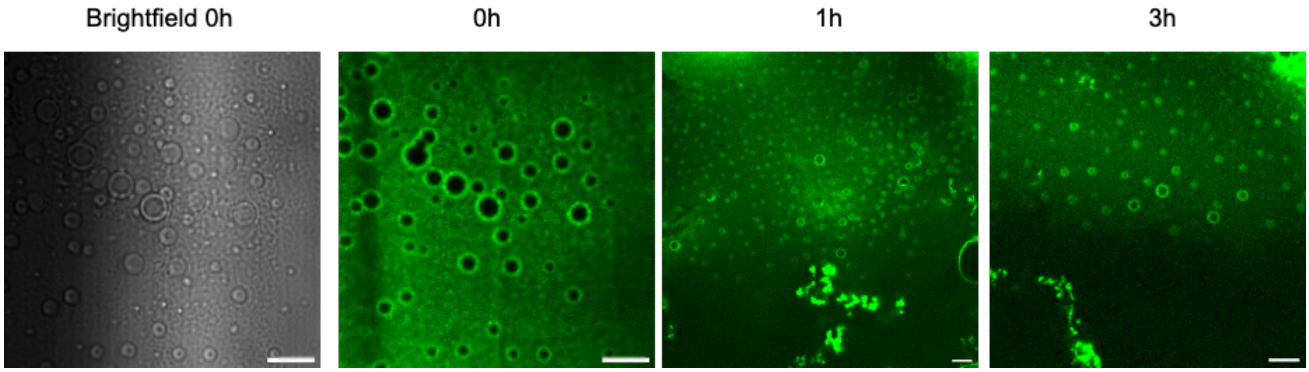

Supplementary Figure 19 – Full field of view of fluorescence confocal images at different timepoints following incubation of the P7 coacervates with Alexa-labeled CotB*p*. Scale bar set to 10µm. The confocal microscopy images are representative images from at least three independently samples with similar results.

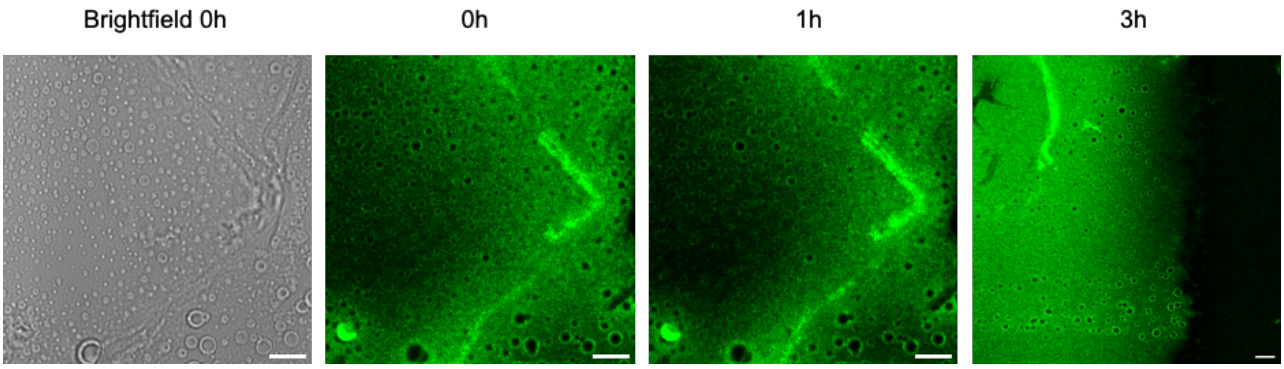

Supplementary Figure 20 – Full field of view of fluorescence confocal images at different timepoints following incubation of the P7 coacervates with Alexa-labelled CotB. Scale bar set to 10µm. The confocal microscopy images are representative images from at least three independently samples with similar results.

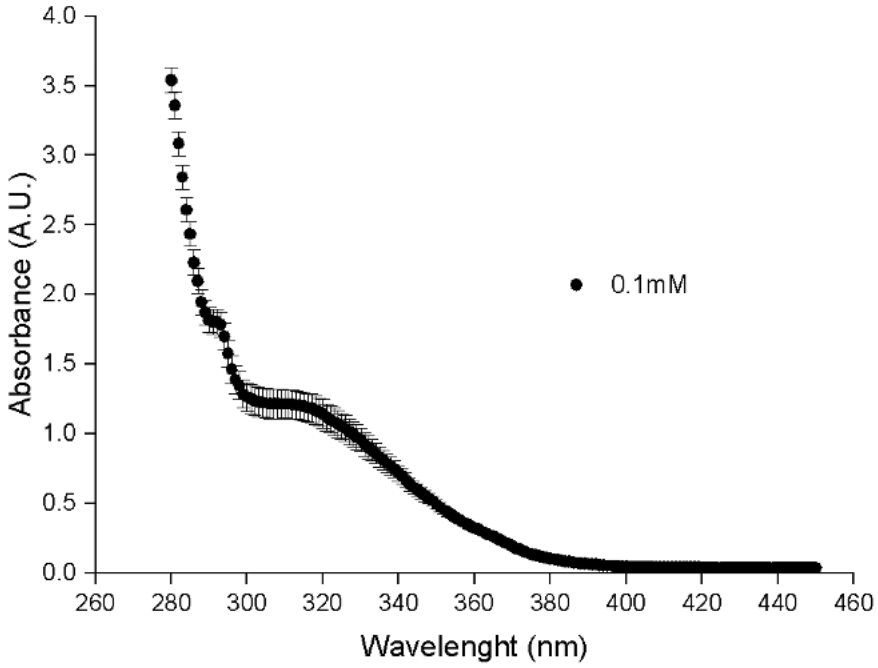

Supplementary Figure 21 Absorbance spectra of the pNPP. Data are presented as mean values ± SD (n = 3) from three independent experiments.

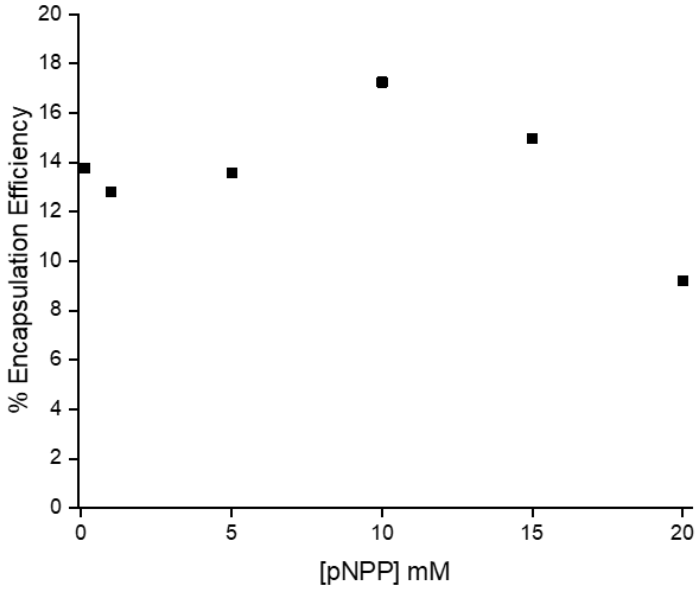

Supplementary Figure 22 Encapsulation efficiency (%) as a function of the pNPP concentration inside P7 coacervates. The encapsulation efficiency was determined by measuring the partitioning of the pNPP within the coacervates. Data are presented as mean values ± SD (n=3) from three independent experiments.

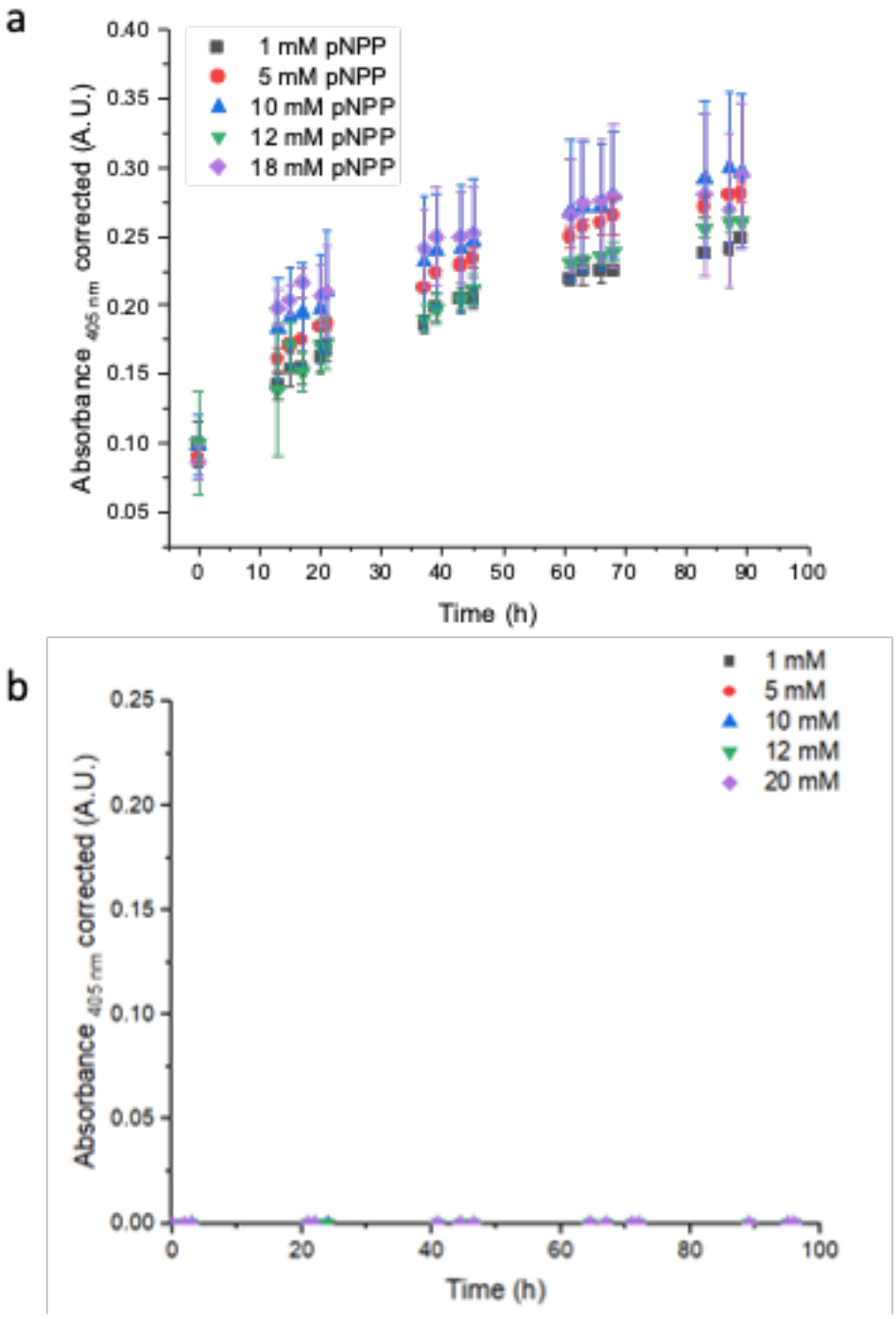

Supplementary Figure 23- The kinetic experiments of the (a) P7 coacervates and (b) P7 bulky solution was carried out by using the phosphatase model substrate pNPP. The hydrolysis of the pNPP by the P7 coacervates and P7 in bulky solution was monitored by the absorbance at 405 nm from the chromogenic product p-nitrophenol for a total of 90h. Data are presented as mean values ± SD (n = 3) from three independent experiments.

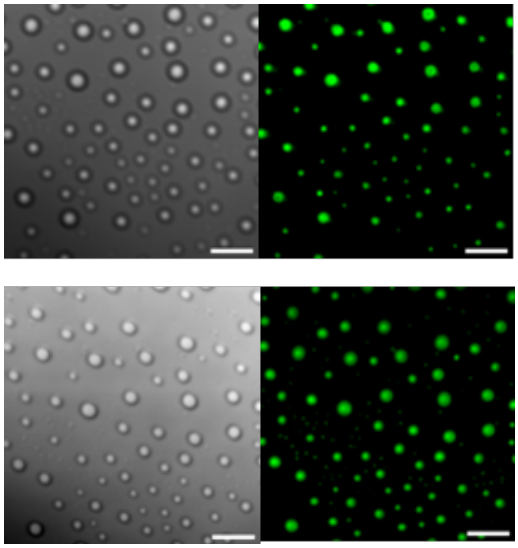

Supplementary Figure 24 - Representative confocal images of the P7 coacervates at 120 hours after incubation with BBTP. Scale bar set to 10µm. The confocal microscopy images are representative images from at least three independently samples with similar results.

6. Supplementary References

1 Freitas, C. *et al.* A protein phosphorylation module patterns the Bacillus subtilis spore outer coat. *Molecular Microbiology* **114**, 934-951 (2020).